Direct ab Initio Dynamics Study on the Hydrogen Abstraction Reaction of $CH_3CCl_3 + OH \rightarrow CH_2CCl_3 + H_2O$

Jing-yao Liu,[†] Ze-sheng Li,*[,†] Zhen-wen Dai,[‡] Xu-ri Huang,[†] and Chia-chung Sun[†]

Institute of Theoretical Chemistry, State Key Laboratory of Theoretical and Computational Chemistry, Jilin University, Changchun 130023, P. R. China, and Department of Physics, Jilin University, Changchun 130023, P. R. China

Received: January 4, 2003; In Final Form: May 15, 2003

The ab initio direct dynamics approach is employed to study the hydrogen abstraction reaction of $CH_3CCl_3 + OH$. The potential energy surface (PES) information is obtained at the MP2/6-311G(d,p) and G3(MP2) (single-point) levels of theory. A hydrogen-bonded complex is located in the reactant channel. Dynamics calculations are performed by variational transition-state theory with the interpolated single-point energy approach (VTST-ISPE). Canonical variational transition-state theory and a small curvature tunneling correction are included to calculate the rate constants within 200−2000 K. Both theoretical rate constants and activation energy are in good agreement with experimental ones over the measured temperature range, 222−761 K. The calculations show that the variational effect is small and the tunneling effect is significant in the lower temperature range.

1. Introduction

It is well-known that halocarbons play a very important role in atmospheric chemistry. Methyl chloroform, i.e., 1,1,1-trichloroethane (CH_3CCl_3), has received considerable attention because of its increased use in industrial degreasing operations as a replacement for the "restricted" solvent trichloroethylene and its well-known connection to the depletion of stratospheric ozone in the ClO_x catalytic cycle.[1] The atmospheric loss of CH_3CCl_3 is due primarily to reaction with OH radical, and the measurements of atmospheric CH_3CCl_3 concentrations have been used to deduce weighted global average tropospheric OH concentrations. This information is important in estimating the atmospheric lifetimes of other reactive atmospheric constituents whose major removal is controlled by OH reactions.[2−6] Therefore, extensive experimental studies[7−18] have been carried out on the title reaction since 1978, especially in the lower temperature regions and at room temperature. However, there is a large discrepancy in these measured rate constants at 298 K. The values of k(298 K) range from 0.95 to 2.5×10^{-14} cm^3 molecule^{-1} s^{-1}. The currently recommended Arrhenius expression of the rate constant is $k = 1.8 \times 10^{-12} \exp(-1550 \pm 150/T)$ cm^3 molecule^{-1} s^{-1}.[19]

The large amount of experimental work on the reaction of $CH_3CCl_3 + OH$ contrasts with the lack of theoretical studies; thus, there have only been three theoretical studies predicting the temperature dependence of the rate constants. These studies employed transition-state theory[20] and empirical models.[21,22] To the best of our knowledge, no ab initio calculations have been carried out on this hydrogen abstraction reaction. Owing to the importance of the reaction, an ab initio investigation is worthwhile. Our study aims to obtain more kinetic information for the title reaction and to evaluate the rate constants over a wide temperature range using the direct dynamics method.[23−25]

* To whom correspondence should be addressed. E-mail: ljy121@mail.jlu.edu.cn.

[†] State Key Laboratory of Theoretical and Computational Chemistry.

[‡] Department of Physics.

2. Calculation Methods

High-level ab initio calculations are carried out with the Gaussian 98 program.[26] The optimized geometries and harmonic vibrational frequencies (scaled by a factor of 0.95) of all the stationary points (the reactants, complex, transition state (TS), and products) are calculated with restricted or unrestricted second-order Møller−Plesset perturbation theory with the standard 6-311G(d,p) basis set ((U)MP2/6-311G(d,p)). To yield a more reliable reaction enthalpy and barrier height, we make single-point energy calculations for the stationary points at the G3(MP2)[27] level of theory (Gaussian-3 (G3) theory[28] with a reduced order of perturbation theory) using the(U)MP2/6-311G(d,p) optimized geometries, since the G3(MP2) method achieves significantly improved accuracy but requires significantly less computational time and disk storage. We also perform higher level single-point energy calculations at the PMP2/6-311++G(3df,3pd), QCISD(T)/6-311G(d,p), and PMP4/6-311G(2d,2p) levels. The intrinsic reaction coordinate (IRC),[29] i.e., minimum energy path (MEP), is calculated at the MP2 level to confirm that the TS really connects with minima along the reaction path. The MEP is calculated in mass-weighted Cartesian coordinates with a gradient step size of 0.05 (amu)$^{1/2}$ bohr. The energy derivatives, including gradients and Hessians at geometries of some selected points (15 points) along the MEP, are calculated at the same level. Furthermore, single-point G3(MP2) calculations of four points along the reaction path are carried out to refine the lower-level energy profile with the interpolated single-point energies (ISPE)[30] approach.

This initial information on the potential energy surface (PES) is used to evaluate rate constants by means of the Polyrate 8.4.1 program.[31] The theoretical rate constants are calculated by using the canonical variational transition theory (CVT)[32] with the small-curvature tunneling (SCT) approximation[33,34] proposed by Truhlar and co-workers. The generalized normal-mode analysis is performed in Cartesian coordinates. The lowest vibrational mode of the transition state is treated as a hindered rotation, and all other vibrations are treated harmonically. The hindered

10.1021/jp034019a CCC: $25.00
Published on Web 07/18/2003

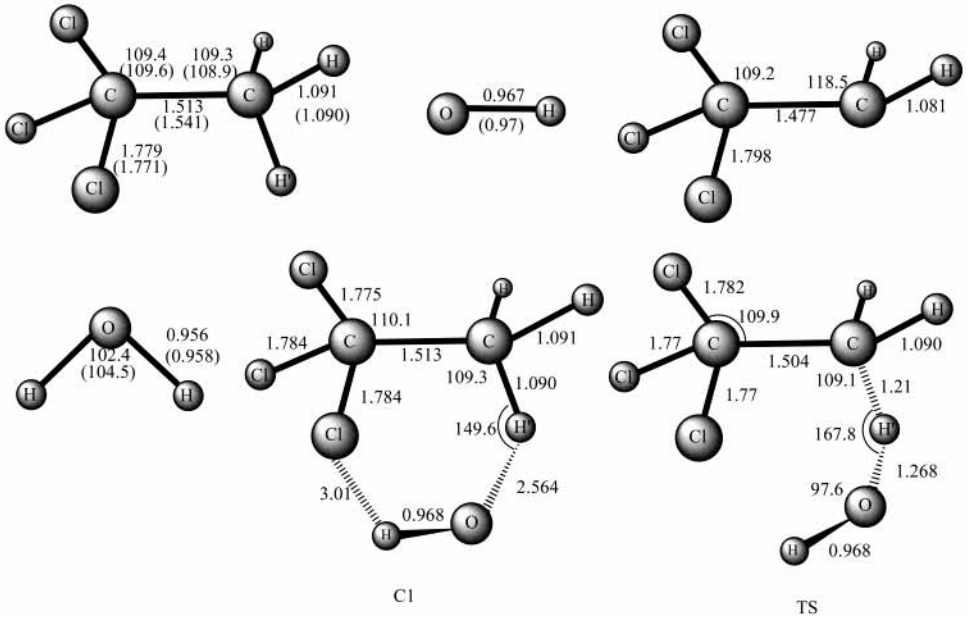

Figure 1. Optimized geometries of all the stationary points at the MP2/6-311G(d,p) level. The values in the parentheses are the experimental values.[36] Bond lengths are in Å and angles are in deg.

TABLE 1: Frequencies (Scaled by 0.95, in cm^{-1}) of Equilibrium and Transition-State Structures at the MP2/6-311G(d,p) Level[a]

species	frequency (cm^{-1})					
CH_3CCl_3	244 (241)	333 (282)	344 (341)	345(346)	519 (525)	730 (725)
	1068 (1074)	1069 (1084)	1367 (1383)	1415 (1450)	2946 (2951)	3046 (3014)
OH	3660 (3735)					
C1	36	56	84	91	257	258
	273	358	362	367	367	544
	761	772	1125	1125	1134	1444
	1490	1495	3101	3204	3212	3840
CH_2CCl_3	181	236	246	320	345	353
	521	581	720	737	1058	1112
	1415	3061	3379			
H_2O	1585 (1595)	3708 (3657)	3839 (3756)			
TS	1950i	61	92	131	223	246
	308	344	347	415	516	702
	718	747	839	1028	1080	1097
	1223	1380	1397	2989	3077	3648

[a] The values in parentheses are experimental values from ref 36 (for OH and H_2O) and ref 37 (for CH_3CCl_3).

rotor approximation[35] is used to calculate the partition function of the lowest vibrational mode. The two electronic states for OH radical are included in the calculation of its electronic partition function, with a 140 cm^{-1} splitting in the $^2\Pi$ ground state. The curvature components of the MEP are calculated by using a quadratic fit to obtain the derivative of the gradient with respect to the reaction coordinate.

3. Results and Discussion

3.1. Stationary Points. At the MP2/6-311G(d,p) level, the optimized geometries of all the stationary points are shown in Figure 1 along with the available experimental data.[36] The corresponding harmonic vibrational frequencies (scaled by 0.95) and the experimental values[36,37] are listed in Table 1. It can be seen that the theoretical values are in good agreement with the experimental ones. The bond lengths of the reactants and products agree with the experimental values within 2%, and the largest deviation of the bond angles is 2° for ∠HOH of H_2O. The scaled frequencies at the MP2 level are in reasonable agreement with the available experimental values except for the calculated value of 333 cm^{-1} of CH_3CCl_3, which differs from the corresponding experimental value of 282 cm^{-1} by about 18%. For the title reaction, a hydrogen-bonded complex (C1), which corresponds to all real frequencies, is located in the reactant channel. In the C1 structure, the O···H′ bond distance is 2.56 Å, and the other bond lengths are very close to those of the reactants. The reactant complex stabilization is of 1.6 kcal/mol with respect to reactants at the G3(MP2)//MP2 level. This indicates that the reaction may proceed via an indirect mechanism, if the system is trapped in the van der Waals well. The transition state is confirmed by verifying that it has only one imaginary frequency. In the transition-state structure, the reactive C−H′ bond is elongated by 11% as compared to the C−H equilibrium bond length of CH_3CCl_3, and the O−H′ bond is 32% longer than the O−H equilibrium bond length of H_2O. Therefore, the transition state is reactant-like, and the reaction will proceed via an "early" transition state.

Because of the limitation of available computational resources, the G3(MP2) method[27] is employed to perform the single-point calculations using the MP2 optimized geometries. For comparison purposes, the single-point energy calculations for the stationary points are also done at other three higher levels, i.e., PMP2/6-311++G(3df,3pd), QCISD(T)/6−311(d,p), and PMP4/6-311G(2d,2p). The values of the reaction enthalpy

TABLE 2: Reaction Enthalpies (ΔH°_{298}) and Barrier Heights ($\Delta E^\ddagger$) (in kcal/mol) with ZPE Corrections for the Reaction at Various Levels[a]

	MP2/6-311G(d,p)	MP2/6-311++G (3df,3pd)// MP2	QCISD(T)/6-311G (d,p)//MP2	PMP4/6-311G (2d,2p)//MP2	G3(MP2)//MP2	exptl[b]
ΔH°_{298}	−12.16 (−12.63)	−17.21 (−17.42)	−9.53	−11.07 (−11.38)	−13.78	−15.59
$\Delta E^\ddagger$	7.72 (5.41)	5.06 (2.64)	6.29	6.57 (5.26)	5.14	

[a] The values in parentheses are the corresponding PMP2 or PMP4 results. [b] The experimental values are from refs 19 and 38.

(ΔH°_{298}) and barrier height ($\Delta E^\ddagger$) with ZPE corrections are listed in Table 2 together with the corresponding experimental values. It is shown that for the reaction system under study the calculated results of ΔH°_{298} and $\Delta E^\ddagger$ are sensitive to the level of electron correlation recovery, and they are even more sensitive to the basis set. The ΔH°_{298} values calculated from MP4 and QCISD(T) results are lower than the corresponding MP2/6-311G(d,p) value by about 1.0 and 2.5 kcal/mol, respectively, while the energy difference amounts to nearly 5 kcal/mol when the size of the basis set is increased from 6-311G(d,p) to 6-311++G(3df,3pd) at the MP2 level. Clearly, the results calculated at the G3(MP2) and MP2/6-311++G-(3df,3pd) levels yield better agreement with the experimental value −15.59 kcal/mol, which is derived from the experimental standard heats of formation (OH, 8.85 kcal/mol;[38] CH_3CCl_3, −34.55 kcal/mol;[19] H_2O, −57.85 kcal/mol;[19] CH_2CCl_3, 16.56 kcal/mol[19]). Compared with the MP2/6-311G(d,p) value, the reaction barrier decreases by 1.43 kcal/mol at the QCISD(T)//MP2 level and by 2.46 kcal/mol at the PMP4//MP2 level, while at the PMP2/6-311++G(3df,3pd) level it is brought down by 5.08 kcal/mol. The G3(MP2) result of $\Delta E^\ddagger$ is in better agreement with those obtained at the PMP4/6-311G(2d,2p) and MP2/6-311++G(3df,3pd) levels, while the PMP2/6-311++G(3df,3pd) level underestimates the potential barrier. It should be noted that the standard G3(MP2) method utilizes the geometry optimized at the MP2(full)/6-31G(d) level, while here we make G3(MP2) single-point calculations using the MP2/6-311G(d,p) geometries. For the title system, the standard G3(MP2) energies of $\Delta H^\circ_{298}$and $\Delta E^\ddagger$ values are very close to those calculated at G3(MP2)//MP2/6-311G(d,p). The former values are slightly lower than the latter ones by about 0.3 and 0.6 kcal/mol, respectively. In addition, it is found that the spin projection correction is more significant for $\Delta E^\ddagger$ than for ΔH°_{298}. The projection of spin contamination lowers the MP2 and MP4 barriers by about 2.4 and 1.3 kcal/mol, respectively, whereas it has a negligible effect on the calculated reaction enthalpies. This is due to the fact that there is more serious spin contamination in the TS with a $\langle S^2\rangle$ value of 0.78 than in OH and CH_2CCl_3 (for which $\langle S^2\rangle$ equals to 0.755 and 0.764, respectively). It is known that the G3(MP2) method[27] is a good compromise between accuracy and computational expense, especially for such larger system. Therefore, in the present study, G3(MP2)//MP2 calculations can be utilized effectively to improve the energies along MEP.

3.2. Reaction Path Properties. By means of a dual-level X//Y calculation method, the minimum energy path is obtained at the MP2/6-311G(d,p) level and the potential profile is further refined with the ISPE method[29] by performing single-point calculations of four extra points ($s = \pm 0.25, \pm 1.25$) along MEP at the G3(MP2) level. The classical potential energy curve ($V_{MEP}(s)$), the vibrationally adiabatic ground-state potential energy curve ($V_a^G(s)$), and the zero-point energy (ZPE) curve of the reaction as a function of the intrinsic reaction coordinate (s) at the G3(MP2)//MP2 level are presented in Figure 2. As can be seen, the $V_{MEP}(s)$ and $V_a^G(s)$ curves are similar in shape, and the positions of the maximum values of the two curves are located at the same position ($s = 0$). This implies that the variational effect will be small for calculating the rate constants of the reaction. The ZPE is practically constant as s varies, with only a gentle drop near the saddle point.

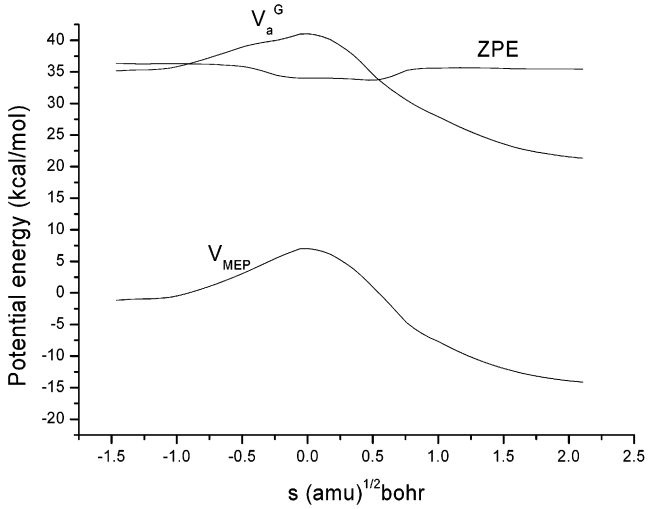

Figure 2. Classical potential energy curve (V_{MEP}), ground vibrationally adiabatic energy curve (V_a^G), and zero-point energy curve (ZPE) as functions of s (amu)$^{1/2}$ bohr at the G3(MP2)//MP2/6-311G(d,p) level.

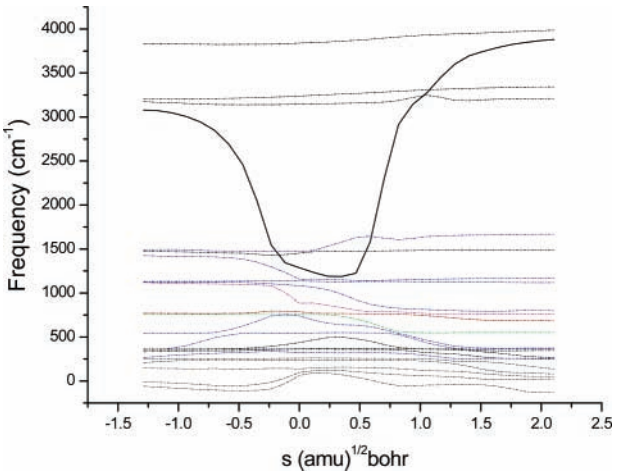

Figure 3. Changes of the generalized normal-mode vibrational frequencies as functions of s (amu)$^{1/2}$ bohr at the MP2/6-311G(d,p) level.

The behavior of the generalized normal-mode vibrational frequencies along the IRC is shown in Figure 3. Most of these frequencies do not change significantly in going from the reactants to products. Hence, these modes are considered as spectator modes, and they involve motions not directly involved in the reaction. The two lowest vibrational frequencies are the transitional modes, which at the asymptote correspond to free rotations and translations of the reactants. Mode 1, shown as the solid line in Figure 3, corresponds to the C−H′ stretching mode at the reactants and the H′−O stretching mode at the products; it drops sharply in the region from $s = -1.0$ to 1.2 (amu)$^{1/2}$ bohr as the reaction proceeds. Therefore, mode 1 can be referred to as the "reactive mode" in the reaction.

TABLE 3: Rate Constants (cm^3 $Molecule^{-1}$ s^{-1}) for the Reaction CH_3CCl_3 + OH at the G3(MP2)//MP2/6-311G(d,p) Level

T (K)	TST	CVT	CVT/SCT	ref 11	ref 13	ref 16	ref 18
200	9.51(−18)[a]	9.48(−18)	3.46(−15)				
222	3.52(−17)	3.50(−17)	4.58(−15)	3.18 ± 0.95(−15)			
233	6.20(−17)	6.17(−17)	5.29(−15)			3.04 ± 0.19(−15)	
243	9.96(−17)	9.89(−17)	6.04(−15)			3.49 ± 0.16(−15)	
252	1.48(−16)	1.47(−16)	6.81(−15)			4.10 ± 0.13(−15)	
253	1.54(−16)	1.53(−16)	6.90(−15)	4.47 ± 1.35(−15)			
263	2.32(−16)	2.30(−16)	7.88(−15)	5.40 ± 1.45(−15)		5.22 ± 0.30(−15)	
273	3.40(−16)	3.36(−16)	9.00(−15)			5.79 ± 0.20(−15)	
278	4.07(−16)	4.03(−16)	9.61(−15)		8.30 ± 0.70(−15)		
293	6.78(−16)	6.69(−16)	1.17(−14)		1.06 ± 0.11(−14)	8.98 ± 0.60(−15)	
296	7.47(−16)	7.36(−16)	1.22(−14)	1.08 ± 0.20(−14)		9.10 ± 0.30(−15)	
297	7.71(−16)	7.60(−16)	1.23(−14)			8.50 ± 0.20(−15)	
298	7.95(−16)	7.84(−16)	1.25(−14)	2.19 ± 0.26(−14)*b*	2.24(−14)[c]	9.5(−15)	1.10 ± 0.10(−14)
326	1.79(−15)	1.76(−15)	1.79(−14)			1.49 ± 0.05(−14)	
352	3.43(−15)	3.36(−15)	2.45(−14)		2.93 ± 0.2(−14)	2.07 ± 0.06(−14)	
363	4.41(−15)	4.31(−15)	2.79(−14)	3.85 ± 0.75(−14)			
370	5.14(−15)	5.02(−15)	3.02(−14)			2.67 ± 0.05(−14)	
379	6.22(−15)	6.06(−15)	3.35(−14)			3.07 ± 0.11(−14)	
400	9.41(−15)	9.13(−15)	4.24(−14)		5.52 ± 0.41(−14)		5.00 ± 1.00(−14)
457	2.46(−14)	2.37(−14)	7.68(−14)		1.02 ± 0.07(−13)		9.40 ± 0.50(−14)
460	2.58(−14)	2.48(−14)	7.91(−14)				1.09 ± 0.29(−13)
495	4.22(−14)	4.05(−14)	1.10(−13)				1.22 ± 0.12(−13)
513	5.33(−14)	5.10(−14)	1.29(−13)				1.27 ± 0.09(−13)
527	6.33(−14)	6.05(−14)	1.46(−13)				1.85 ± 0.13(−13)
535	6.97(−14)	6.65(−14)	1.56(−13)				2.02 ± 0.10(−13)
560	9.26(−14)	8.82(−14)	1.92(−13)				2.18 ± 0.28(−13)
601	1.42(−13)	1.35(−13)	2.61(−13)				2.35 ± 0.38(−13)
642	2.08(−13)	1.97(−13)	3.49(−13)				3.31 ± 0.81(−13)
671	2.68(−13)	2.52(−13)	4.23(−13)				3.68 ± 0.36(−13)
720	3.95(−13)	3.70(−13)	5.74(−13)				5.45 ± 0.20(−13)
761	5.32(−13)	4.96(−13)	7.28(−13)				7.26 ± 0.39(−13)
800	6.91(−13)	6.42(−13)	9.01(−13)				
1000	2.09(−12)	1.91(−12)	2.28(−12)				
1200	4.82(−12)	4.32(−12)	4.77(−12)				
1500	1.25(−11)	1.10(−11)	1.13(−11)				
2000	3.85(−11)	3.29(−11)	3.23(−11)				

[a] 9.51(−18) stands for 9.51×10^{-18}. [b] From ref 9. [c] From ref 10.

3.3. Rate Constant Calculations. The rate constants are calculated by the canonical variational transition state theory[31] with a small-curvature tunneling correction[32,33] (CVT/SCT) at the G3(MP2)//MP2/6-311G(d,p) level over a wide temperature range, 200−2000 K. For the purpose of comparison, the conventional transition state theory (TST), CVT, and CVT/SCT rate constants are presented in Table 3 as well as the available experimental values. The variational effect, that is, the ratio between the variational CVT and conventional TST rate constants, goes from a value of 0.99 at 200 K to a value of 0.85 at 2000 K. Therefore, for the reaction under consideration, the variational effect is small over the whole temperature range. Moreover, Figure 4 shows that the tunneling effect plays an important role in rate constant calculations, in particularly, in the lower temperature range. The ratio of the CVT/SCT rate constants to the CVT rate constants increases rapidly from a value of 1.4 at 800 K to 365 at 200 K.

The CVT/SCT rate constants and available experimental values are plotted against 1000/*T* (K) in Figure 4. The CVT/SCT rate constants are in good agreement with the corresponding experimental values[11,13,16−19] over the measured temperature range 222−761 K if the experimental uncertainties are taken into account. The calculated results slightly overestimate the experimental values of Talukdar et al.,[16] while they are slightly higher than those reported by Kurylo et al.[11] and Jeong et al.[13] in the range 352−400 K. The deviation remains within a factor of 1.1 to 1.7. At 298 K, the CVT/SCT rate constant (1.25×10^{-14}) shows better consistency with the experimental value of (1.1 ± 0.1) $\times 10^{-14}$ determined by Jiang et al.[18] In the temperature region 400−761 K, our calculations reproduce quite well the experimental rate constants.[18] The Arrhenius expression was fitted by the CVT/SCT rate constants, and this yields $k = 5.9 \times 10^{-12} \exp(-1923/T)$ cm^3 $molecule^{-1}$ s^{-1} in the temperature range 298−761 K. The calculated activation energy from this fit, 3.8 kcal/mol, is in good accord with the experimental value, 3.1 ± 0.3 kcal/mol, which is derived from the currently recommended expression $k = 1.8 \times 10^{-12} \exp[(-1550 \pm 150)/T]$ cm^3 $molecule^{-1}$ s^{-1}.[19] The good agreement between theory and experiments obtained at the G3(MP2)//MP2/6-311G(d, p) level indicates that present calculations can provide reasonable

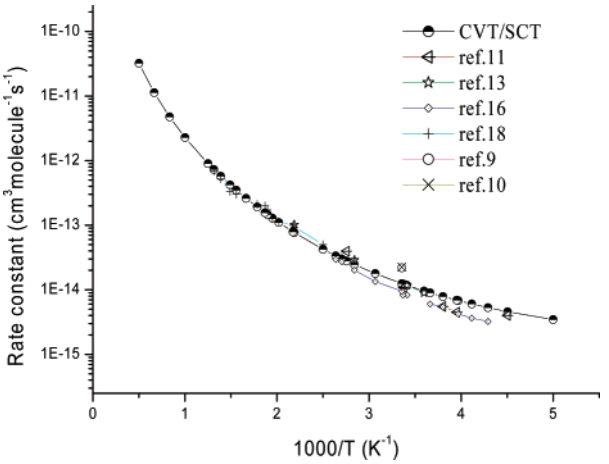

Figure 4. Plot of the calculated rate constants (cm^3 $molecule^{-1}$ s^{-1}) at the G3(MP2)//MP2/6-311G(d,p) level and available experimental values vs 1000/*T* in 200−2000 K.

predictions for the title reaction at higher temperatures. Thus, to further describe the non-Arrhenius behavior of the rate constants, the three-term expression of the type $AT^m \exp(-b/T)$ was fit to the CVT/SCT calculations. This yields $k = 2.53 \times 10^{-25} T^{4.3} \exp(70/T)$ cm^3 molecule^{-1} s^{-1} over the wide temperature range 200−2000 K.

4. Conclusion

In this paper, the hydrogen abstraction reaction of CH_3CCl_3 by OH has been investigated by the ab initio direct dynamics method. A hydrogen-bonded complex is present on the reactant side, indicating that the reaction may proceed via an indirect mechanism. The geometries, first derivatives, and frequencies of the stationary points and points along the reaction path are obtained at the MP2/6-311G(d,p) level of theory. A few of single-point energy calculations are carried out by the G3(MP2) method to improve the energy profile along the minimum energy path calculated at the lower level. The rate constants are calculated by using variational transition-state theory with the interpolated single-point energies (VTST-ISPE) method. The small-curvature tunneling contribution is included. Our calculations show that agreement with the experimental results both for the rate constants and for the activation energy is good. Three-parameter fits to the CVT/SCT rate constants for the reaction over the interval 200−2000 K give the expression of $k = 2.53 \times 10^{-25} T^{4.3} \exp(70/T)$ cm^3 molecule^{-1} s^{-1}. It is expected that the present theoretical study may be useful for estimating the kinetics of the reactions over a wide temperature range where no experimental data are available.

Acknowledgment. We thank Professor Donald G. Truhlar for his provision of the POLYRATE 8.4.1 program. This work is supported by the National Natural Science Foundation of China (Grant 20073014), Doctor Foundation by the Ministry of Education, Foundation for University Key Teacher by the Ministry of Education, Key Subject of Science and Technology by the Ministry of Education of China, and the Innovational Foundation by Jilin University.

References and Notes

(1) Crutzen, P. J.; Isaksen, I. A.; McAfee, J. R. *J. Geophys. Res.* **1978**, *83*, 345.
(2) Prather, M.; Spivakovsky, C. M. *J. Geophys. Res.* **1990**, *95*, 18723.
(3) Zhang, Z.; Saini, R. D.; Kurylo, M. J.; Huie, R. E. *J. Phys. Chem.* **1992**, *96*, 9301.
(4) Zhang, Z.; Padmaja, S.; Saini, R. D.; Huie, R. E.; Kurylo, M. J. *J. Phys. Chem.* **1994**, *98*, 4312.
(5) Barry, J.; Locke, G.; Scollard, D.; Sidebottom, H.; Treacy, J.; Clerbaux, C.; Colin, R.; Franklin, J. *Int. J. Chem. Kinet.* **1997**, *29*, 607.
(6) Hus, K.-J.; DeMore, W. B. *J. Phys. Chem.* **1995**, *99*, 1235.
(7) Howard, C. J.; Evenson, K. M. *J. Chem. Phys.* **1976**, *64*, 4303.
(8) Watson, R. T.; Machado, G.; Conaway, B.; Wagnar, S.; Davis, D. D. *J. Phys. Chem.* **1977**, *81*, 256.
(9) Chang, J. S.; Kaufman, F. *J. Chem. Phys*. **1977**, *66*, 4989.
(10) Clyne, M. A. A.; Holt, P. M. *J. Chem. Soc., Faraday Trans. 2* **1979**, *75*, 569.
(11) Kurylo, M. J.; Anderson, P. C.; Klais, O. *Geophys. Res. Lett.* **1979**, *6*, 760.
(12) Jeong, K. M.; Kaufman, F. *Geophys. Res. Lett.* **1979**, *6*, 757.
(13) Jeong, K. M.; Hus, K. J.; Jeffries, J. B.; Kaufman, F. *J. Phys. Chem.* **1984**, *88*, 1222.
(14) Atkinson, R. *J. Phys. Chem. Ref. Data* **1989**, *Monograph 1*, 1.
(15) Nelson, L.; Shanahan, I.; Sidebottom, H. W.; Treacy, J.; Nielsen, O. J. *Int. J. Chem. Kinet.* **1990**, *22*, 577.
(16) Talukdar, R. K.; Mellouki, A.; Schmoltner, A.; Watson, T.; Montzka, S.; Ravishankara, A. R. *Science* **1992**, *257*, 227.
(17) Finlayson-Pitts, B. J.; Ezell, M. J.; Jayaweera, T. M.; Berko, H. N.; Lai, C. C. *Geophys. Res. Lett.* **1992**, *19*, 1371.
(18) Jiang, Z.; Taylor, P. H.; Dellinger, B. *J. Phys. Chem.* **1992**, *96*, 8961.
(19) DeMorse, W. B.; Sander, S. P.; Golden, D. M.; Hampson, R. F.; Kurylo. M. J.; Howard, C. J.; Ravishankara, A. R.; Kolb, C. E.; Molina, M. J.; *Chemical Kinetics and Photochemical Data for use in Stratospheric Modeling, Evaluation*; JPL Publication 94-26; Jet Propulsion Laboratory, California Institute of Technology: Pasadena, CA, 1994.
(20) Cohen, N.; Benson, S. W. *J. Phys. Chem.* **1987**, *91*, 162.
(21) Atkinson, R. *Int. J. Chem. Kinet.* **1986**, *18*, 555.
(22) Cohen, N.; Benson, S. W. *J. Phys. Chem.* **1987**, *91*, 171.
(23) Truhlar, D. G. Direct Dynamics Method for the Calculation of Reaction Rates. In *The Reaction Path in Chemistry: Current Approaches and Perspectives*: Heidrich, D., Ed.; Kluwer: Dordrecht, The Netherlands, 1995; pp 229−255.
(24) Truhlar, D. G.; Garrett, B. C.; Klippenstein, S. J. *J. Phys. Chem*. **1996**, *100*, 12771.
(25) Hu, W. P.; Truhlar, D. G. *J. Am. Chem. Soc*. **1996**, *118*, 860.
(26) Frisch, M. J.; Truck, G. W.; Schlegel, H. B.; Scuseria, G. E.; Robb, M. A.; Cheeseman, J. R.; Zakrzewski, V. G.; ontgomery, J. A., Jr.; Stratmann, R. E.; Burant, J. C.; Dapprich, S.; Millam, J. M.; Daniels, A. D.; Kudin, K. N.; Strain, M. C.; Farkas, O.; Tomasi, J.; Barone, V.; Cossi, M.; Cammi, R.; Mennucci, B.; Pomelli, C.; Adamo, C.; Clifford, S.; Ochterski, J.; petersson, G. A.; Ayala, P. Y.; Cui, Q.; Morokuma, K.; Malick, D. K.; Rabuck, A. D.; Raghavachari, K.; Foresman, J. B.; Cioslowski, J.; Ortiz, J. V.; Boboul, A. G.; Stefnov, B. B.; Liu, G.; Liaschenko, A.; Piskorz, P.; Komaromi, L.; Gomperts, R.; Martin, R. L.; Fox, D. J.; Keith, T.; Al-Laham, M. A.; Peng, C. Y.; Nanayakkara, A.; Gonzalez, C.; Challacombe, M.; Gill, P. M. W.; Johson, B.; Chen, W.; Wong, M. W.; Andres, J. L.; Gonzalez, C.; Head-Gordon, M.; Replogle, E. S.; Pople, J. A. *Gaussian 98*, G98W A.7; Gaussian, Inc.: Pittsburgh, PA, 1998.
(27) Curtiss, L. A.; Redfern, P. C.; Raghavachari, K.; Rassolov, V.; Pople, J. A. *J. Chem. Phys.* **1999**, *110*, 4703.
(28) Curtiss, L. A.; Raghavachari, K.; Redfern, P. C.; Rassolov, V.; Pople, J. A. *J. Chem. Phys.* **1998**, *109*, 7764.
(29) (a) Gonzalez, C.; Schlegel, H. B. *J. Chem. Phys.* **1989**, *90*, 2154. (b) Gonzalez, C.; Schlegel, H. B. *J. Phys. Chem.* **1990**, *94*, 5523.
(30) Chuang, Y.-Y.; Corchado, J. C.; Truhlar, D. G. *J. Phys. Chem.* A **1999**, *103*, 1140.
(31) Chuang, Y.-Y.; Corchado, J. C.; Fast, P. L.; Villa, J.; Hu, W. P.; Liu, Y.-P.; Lynch, G. C.; Jackels, C. F.; Nguyen, K. A.; Gu, M. Z.; Rossi, I.; Coitino, E. L.; Clayton, S.; Melissas, V. S.; Lynch, B. J.; Steckler, R.; Garrett, B. C.; Isaacson, A. D.; Truhlar, D. G. *POLYRATE*, version 8.4.1; University of Minnesota: Minneapolis, MN, 2000.
(32) Garrett, B. C.; Truhlar, D. G. *J. Chem. Phys.* **1979**, *70*, 1593.
(33) Lu, D.-H.; Truong, T. N.; Melissas, V. S.; Lynch, G. C.; Liu, Y.-P.; Garrett, B. C.; Steckler, R.; Issacson, A. D.; Rai, S. N.; Hancock, G. C.; Lauderdale, J. G.; Joseph, T.; Truhlar, D. G. *Comput. Phys Commun*. **1992**, *71*, 235.
(34) Liu, Y.-P.; Lynch, G. C.; Truong, T. N.; Lu, D.-H.; Truhlar, D. G. *J. Am. Chem. Soc*. **1993**, *99*, 1013.
(35) Chuang, Y.-Y.; Truhlar, D. G. *J. Chem. Phys.* **2000**, *112*, 1221.
(36) Chase, M. W., Jr. NIST-JANAF Themochemical Tables, 4th edition. *J. Phys. Chem. Ref. Data* **1998**, Monograph 9.
(37) Frankiss, S. G.; Harrison, D. J. *Spectrochim. Acta* A **1975**, *31A*, 29.
(38) (a) Ruscic, B.; Feller, D.; Dixon, D. A.; Peterson, K. A.; Harding, L. B.; Asher, R. L.; Wagner, A. F. *J. Phys. Chem. A* **2001**, *105*, 1. (b) Joens, J. A. *J. Phys. Chem. A* **2001**, *105*, 11041. (c) Ruscic, B.; Wagner, A. F.; Harding, L. B.; Asher, R. L.; Feller, D.; Dixon, D. A.; Peterson, K. A.; Song, Y.; Qian, X.; Ng, C. Y.; Liu, J.; Chen, W.; Schwenke, D. W. *J. Phys. Chem. A* **2002**, *106*, 2727.